ACS APPLIED MATERIALS & INTERFACES

Research Article

www.acsami.org

Palladium Nanoparticle-Based Surface Acoustic Wave Hydrogen Sensor

Devika Sil,[†] Jacqueline Hines,[‡] Uduak Udeoyo,[†] and Eric Borguet*[,†]

[†]Department of Chemistry, Temple University, 1901 North 13th Street, Philadelphia, Pennsylvania 19122, United States

[‡]SenSanna Incorporated, Arnold, Maryland 21012, United States

Supporting Information

ABSTRACT: Palladium (Pd) nanoparticles (5−20 nm) are used as the sensing layer on surface acoustic wave (SAW) devices for detecting H_2. The interaction with hydrogen modifies the conductivity of the Pd nanoparticle film, producing measurable changes in acoustic wave propagation, which allows for the detection of this explosive gas. The nanoparticle-based SAW sensor responds rapidly and reversibly at room temperature.

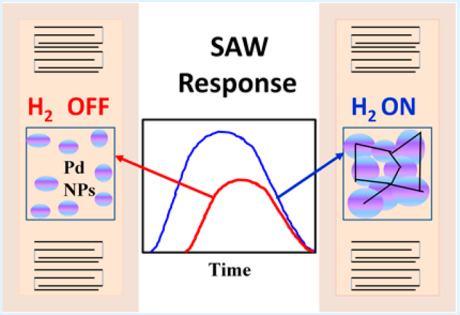

KEYWORDS: *hydrogen, surface acoustic, sensing, reversible, conductivity*

INTRODUCTION

Hydrogen is a carbon-free fuel with important applications, but there are serious risks involved with its use. It is an asphyxiant, as well as explosive and extremely flammable in air. Furthermore, being colorless and odorless, it is difficult to detect. To limit the hazards associated with this potentially explosive gas, reliable detectors are required to rapidly sense H_2 at concentrations below regulatory limits and to aid in its detection and containment in response to accidental releases. Hence, dependable hydrogen sensors are imperative to ensure a safe working environment in hydrogen production plants, H_2 refueling stations, H_2 powered cars, petrochemical and metallurgical plants, nuclear power stations, coal mines, and the semiconductor industry.[1] The presence of hydrogen in human breath may also be an indicator of lactose intolerance, fructose malabsorption, neonatal necrotizing enterocolitis, or diabetic gastroparesis, which makes the use of hydrogen sensors biomedically significant.[2] This ubiquitous need for hydrogen detection therefore motivates research directed toward the development of a fast, reusable, and dependable hydrogen sensor.

Traditional hydrogen sensors typically employ microelectromechanical systems (MEMS), catalytic, thermal, electrochemical (resistance and work function), mechanical, optical, and acoustic detection schemes.[1,4] The relative advantages and disadvantages of each type of sensor are discussed in detail elsewhere.[1] In the present work, a special type of acoustic sensor, a Surface Acoustic Wave (SAW) device, will be considered because it is small, offers a passive, wireless sensing platform, and when coated with an appropriate chemically selective layer, may function as a chemical vapor sensor with extremely high sensitivity.[4]

SAW devices are fabricated on a piezoelectric substrate with interdigitated transducers (IDTs) (Figure 1) that convert electrical signals into acoustic waves and vice versa. A chemical sensing layer is deposited on the delay line in between two or more IDTs.[4,5] A high frequency (250 MHz) acoustic wave is

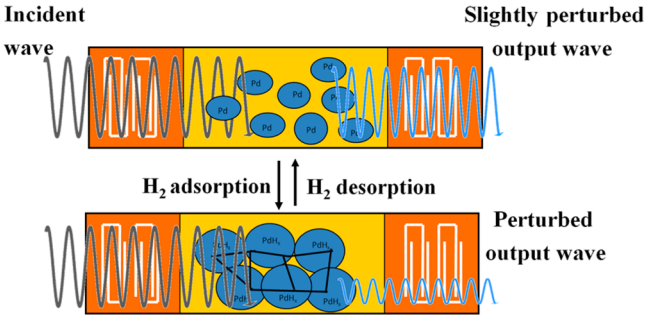

Figure 1. Working principle of a SAW device. In the absence of H_2, an acoustic wave travels through the Pd layer (which has a baseline conductivity that can be varied based on film fabrication processes) with nominal perturbation. Exposure to H_2 induces lattice expansion in Pd so that the nanoparticles become closer together and/or touch and enhance conducting pathways. Any modification in the conductive properties of the Pd sensing film attenuates and perturbs the acoustic wave. The perturbation is reflected as a change in delay and amplitude (insertion loss) of the output acoustic wave detected. Depending on the initial baseline conductivity of the film, exposure to hydrogen can cause an increase or decrease in signal amplitude.

Received: October 29, 2014
Accepted: February 6, 2015
Published: March 6, 2015

DOI: 10.1021/am507531s
ACS Appl. Mater. Interfaces 2015, 7, 5709−5714

launched from one transducer, propagates across the surface of the device passing the sensitive layer before being detected from the second electrode transducer.[4,5] Alternatively, a reflective operation mode can be used (and is the device design employed in this study), wherein the acoustic wave launched from the first transducer propagates across the surface of the device, past the sensitive layer region, and is reflected from the second interdigitated transducer, causing the wave to propagate back under the sensitive layer for a second time before it is received by the launching transducer, doubling the interaction time of the wave with the sensitive layer and enhancing the device sensitivity (Supporting Information, SI, Figure S3).[4,5]

Any physical/chemical/electrical modification in the region close to the surface of the substrate, or of the sensing film, will perturb the propagating acoustic wave (Figure 1) and alter its velocity, phase, and/or amplitude. These modifications are observed as changes in the radio frequency response. Surface acoustic waves are sensitive to changes in the mass loading,[6] viscoelastic properties,[7] and/or electrical conductivity of the sensing layer.[6,8] Therefore, the selection of material for the sensing film is crucial in achieving high detection sensitivity.[4]

An optimum hydrogen sensing material is one which possesses high absorption capacity per unit mass and volume, requires a low H_2 dissociation temperature and moderate dissociation pressure. Additionally, an ideal H_2 sensor should be reversible, and reusable with high stability against oxidation and moisture for long cycle life.[9] Bulk palladium can absorb about 900 times its own volume of hydrogen at room temperature and atmospheric pressure. Furthermore, the dissociation of H_2 on Pd is known to be thermodynamically favored, even with a barrier to hydrogen adsorption of ∼0.2 eV,[10] as the energy of adsorption of H_2 on a clean Pd (111) is calculated to be close to 0.56 eV,[10] with a temperature independent high initial sticking coefficient.[11] Incorporation of hydrogen into Pd causes the formation of PdH_x which is known to exist into two different phases: the α and β phase.[12−14] The α-PdH_x exists in low hydrogen concentration when $x < 0.03$, whereas the β phase is found at higher hydrogen concentrations at $x < 0.6$.[12,14] Experimental evidence suggests that the α phase is dominant at temperatures >50 °C, whereas the β phase exists at lower temperatures because the Pd−H formation occurs via the following processes: (i) physisorption of H_2, (ii) chemisorption and dissociation of hydrogen on the surface, (iii) introduction of hydrogen atoms on the Pd surface, (iv) diffusion of H atoms into the bulk, and (v) palladium hydride formation.[12,15] The absorption of hydrogen causes strain in the lattice of Pd due to the formation of PdH_x with an increased lattice constant (∼3−4%) and volume (∼10%).[16] The structural and morphological modification in Pd due to hydrogen is commonly referred to as Hydrogen Induced Lattice Expansion (HILE).[14,17,18] The lattice expansion may also induce changes in electrical properties, e.g., conductivity, which often forms the basis of hydrogen sensing using Pd.[19−21] Thus, the thermodynamically favored dissociation of hydrogen and reversible lattice expansion justifies the selection of Pd as the sensing material for hydrogen gas detection.

Pd thin films[22−24] and Pd bilayer structures[25,26] have been previously used on SAW devices for sensing hydrogen. However, their drawbacks include the need of sophisticated deposition equipment, like sputter coaters or electron beam evaporators, which typically require vacuum and expensive targets. Additionally, the thin films suffer from hysteresis in electrical resistance during H_2 adsorption and desorption cycles, which is dependent on the film thickness and can be significantly reduced at thicknesses below 5 nm.[27] Attaining such precise dimensions may be challenging and the sensitivity and mechanical stability of such devices are also compromised.[27] Previous scanning tunneling microscopy studies revealed that the crystallites are loosely connected in the nanoparticle samples whereas the thin film samples are more continuous in nature.[28] The interparticle distance in nanoparticle films provides space for hydrogen induced morphological changes whereas the Pd−Hydrogen interaction builds up stress in the thin films due to lack of the interparticle voids, thereby affecting the performance of Pd thin film based sensors. Pd nanoparticle films on the other hand have higher surface to volume ratio hence providing more adsorption sites, which allows the hydrogen to diffuse in and out more readily, increasing the rate at which the sensor can respond to a change in hydrogen vapor concentration and reducing hysteresis. Moreover, in the case of Pd nanoparticles the binding energy of the Pd 4d band is decreased by 0.6 eV, so the miscibility gap is lowered, and a new set of surface and subsurface adsorption sites in addition to the regular interstitial and grain boundary sites for hydrogen adsorption have been reported to appear, enhancing the hydrogen sensing properties.[12,28−35] The Pd nanoparticles are coated with polyvinylpyrrolidone to prevent aggregation, and serve as a protective layer against oxidation. The functioning of the sensor depends on the sensing film and as long as the Pd nanoparticle film can withstand oxidation, the sensors are expected to be durable. All of the aforementioned properties make Pd nanoparticles a promising material in comparison to thin films of Pd for hydrogen sensing.

One of the key challenges faced in the fabrication of nanoparticle based devices is the lack of precise control of size distribution of nanoparticles, as smaller particles are expected to have more adsorption sites. However, when hydrogen sensors fabricated on a non SAW sensing platform with thin films are compared with those that use nanoparticle films of Pd, the latter reflect faster response times and increased sensitivity.[27] A few related reports of nanoparticles on SAWs for hydrogen sensing point toward the usage of Pd nanoparticles coated with Tobacco Mosaic Virus,[36] WO_3 nanoparticles,[37] Pd nanopillars,[38] Pt coated ZnO nanorods,[39] titania nanotubes,[40] isolated samarium nanoparticles,[41] and nanoclusters of titanium benzene complexes.[42] However, the majority of these studies investigated mass loading effects on SAW whereas the Pd nanoparticle based SAW sensor disclosed here exploits the formation/modification of conductive pathways due to electrical contacts either in an Ohmic transport regime, when actual mechanical contact between particles becomes possible following lattice expansion, or in a quantum mechanical tunneling regime, where the electron density distributions overlap.

The nanoparticles utilized for the present study were synthesized using a solution based reduction of H_2PdCl_4 with ethanol under reflux conditions method proposed by Teranishi et al. resulting in 5−20 nm polyvinylpyrrolidone (PVP) capped Pd nanoparticles.[43] The removal of the organic capping layer was considered crucial for exposing the catalytically active Pd sites[44,45] and also for the formation of electrical contact[46] so the films were ozone cleaned prior to hydrogen exposure.

The Pd nanoparticles were characterized using Transmission Electron Microscopy (TEM). Thin films of the Pd nanoparticles were prepared by drop casting followed by ozone

DOI: 10.1021/am507531s
ACS Appl. Mater. Interfaces 2015, 7, 5709−5714

cleaning for measuring the conductivity in situ, both in the presence and absence of hydrogen, to detect the changes in conductive properties brought about by the reversible formation of PdH_x. After identifying the optimal hydrogen sensitive Pd films, similar films were deposited on SAW devices for testing the real-time response to hydrogen.

RESULTS AND DISCUSSION

In Situ Conductivity Measurement. In situ conductivity measurements of Pd nanoparticle films carried out using a scanning tunneling microscopy (STM) test setup (SI Figure S2), indicated changes in the electrical properties in the presence of hydrogen (Figure 2). Initially, the films used for

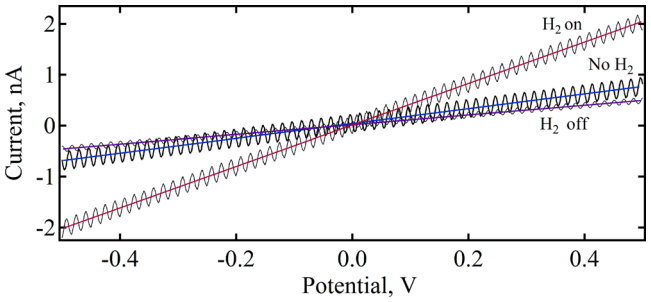

Figure 2. I–V response of a multilayer Pd nanoparticle film (prepared from 25 mM Pd nanoparticle solution, details of film preparation and measurement procedure are described in the SI) measured using an STM preamplifier before, during, and after exposure to 4% H_2 in N_2. The oscillation in the raw data arise from the external noise as the STM preamplifier used for measuring the conductivity is very sensitive. All the three traces; No H_2, H_2 on, and H_2 off are fitted with straight lines (solid lines) Current increased due to H_2 exposure and reversibly decreased after H_2 was shut off recovering to close to the initial level.

these measurements were not highly conductive, hence a STM preamplifier was used as a tool to measure the low currents (10 pA–100 nA and resistance 100 GΩ–10 MΩ). Hydrogen induced lattice expansion caused the nanoparticles to expand leading to the formation of conductive pathways, which causes the current to increase from the baseline value (Figure 2). As hydrogen desorbed, the nanoparticles relaxed back to their original configurations breaking the conductive pathways hence causing the current to decrease again (Figure 2). Thus, the Pd nanoparticle films were conductive at room temperature and underwent reversible expansion in the presence of hydrogen.

Characterization of SAW Sensor Response. The hydrogen sensing properties of Pd nanoparticle coated SAW devices were investigated by exposing the fabricated sensors to a nitrogen purge followed by a mix of 1600 ppm (0.16%) H_2 in N_2 for 5 min, and then a postexposure N_2 purge. A typical time domain response for the reflective SAW delay line device (Figure 3) showed the first, largest peak, the reference response, which did not change regardless of the presence or absence of hydrogen. The peak at ~4 μs, the Rayleigh SAW sensing response, was sensitive to hydrogen. Relative to a SAW device without a sensing film, the sensing peak response was perturbed by the presence of the Pd nanoparticle film, and by exposure to hydrogen. Additional peaks (Figure 3) are due to multiple transit responses of the reference response and the reflected wave (at 0.8 μs, 1.4 μs, 4.7 μs, and 5.3 μs), and acoustic reflections and mode conversions (other peaks with 70 dB and higher insertion loss) from the Rayleigh SAW into other acoustic wave modes. Multiple transit responses were

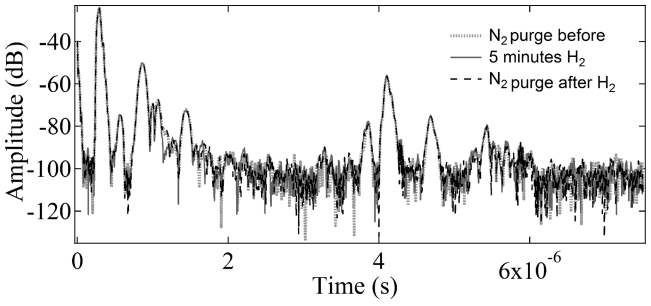

Figure 3. A typical time domain response for the reflective SAW delay line device. The entire response from a single layer Pd SAW device showing reference peak (first peak at 0.28 μs), several peaks for multiple reflections within SAW and mode conversion (3.8 μs), and sensing response peak at approximately 4.1 μs.

expected as the acoustic wave could be regenerated and travel between transducers more than once, but other reflections and modes were undesirable. These undesired responses were present because the sensors did not have any acoustic absorber or backside roughening on the die to eliminate such signals.

The overall time domain response for an open circuit, single and double layer Pd nanocluster film device was recorded before, during, and after exposure to 1600 ppm (0.16%) H_2 in N_2. The reference peak did not change during N_2 purge and hydrogen exposure (SI Figure S4a,c), whereas for the sensing peak (Figure 4) the insertion loss (IL) decreased with exposure to hydrogen, a change which was fully reversible as shown by the response returning to its starting value when the hydrogen gas was removed. A much larger, albeit somewhat noisier, response was obtained for an open circuit, two layer Pd nanocluster film device (Figure 4b) before, during, and after exposure to 0.16% (1600 ppm) H_2 in N_2 (for 3 successive cycles of 5, 6, and 7 min). The H_2 sensitive portion of the device exhibited a decrease in IL of almost 3 dB (indicating a signal level that is nearly double in amplitude on a linear scale) and a large reduction in delay of about 50 ns when exposed to 0.16% (1600 ppm) H_2 in N_2. The decrease in insertion loss is due to reduction in SAW attenuation as film conductivity increases. The increase in film conductivity tends to reduce SAW velocity, yet the responses in Figure 4 show shorter delays with hydrogen exposure, indicating an overall increase in SAW velocity. Thus, there must also be a change in film stiffness upon exposure to hydrogen vapor, causing SAW velocity to increase (reducing signal delay). The magnitude of the change in response to hydrogen was identical in all the three cycles and the response returned to the original value after hydrogen was turned off and purged with nitrogen. Thus, it could be concluded that these Pd based SAW devices are stable over the short-term to multiple cycling of H_2 with little or no hysteresis. Moreover, subsequent to the 0.16% H_2 in N_2 exposure, the same film was also exposed to 8% H_2 in N_2, whereby the H_2 sensitive portion showed a 1 dB increase in IL relative to the IL exhibited in the 1600 ppm hydrogen gas. This result at first appears anomalous, as many sensors respond to increasing gas concentrations with increased sensor response levels. However, SAW sensors that are responsive to film conductivity exhibit a distinct attenuation peak at a specific value of film conductivity, with films that are either more resistive or less resistive than this value causing lower attenuation (Figure 5) resulting in lower IL. Increasing vapor concentration causes the film conductivity to increase for the nanocluster Pd films developed here. Film

DOI: 10.1021/am507531s
ACS Appl. Mater. Interfaces 2015, 7, 5709–5714

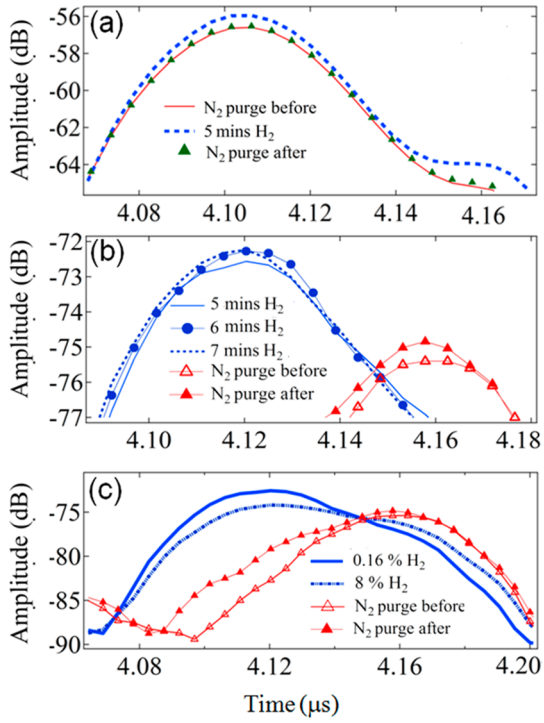

Figure 4. Measured time domain response of SAW sensor with nonmetallized open circuit propagation path with single and double layer Pd nanoparticle coating before, during, and after exposure hydrogen. Sensing response peak enlarged for (a) one layer Pd device during initial N_2 purge, 0.16% H_2 exposure, and postexposure N_2 purge, (b) double layer Pd nanoparticle coated SAW device during initial N_2 purge, 0.16% H_2 exposure for 5, 6, and 7 min successively, and postexposure N_2 purge, and (c) double layer Pd nanoparticle coated SAW device exposed to N_2 purge, 0.16% and 8% H_2 in N_2 for 5 min and postexposure N_2 purge. The sensing peak showed a decrease in insertion loss (IL) during H_2 exposure, and returned to initial N_2 purge levels during postexposure N_2 purge.

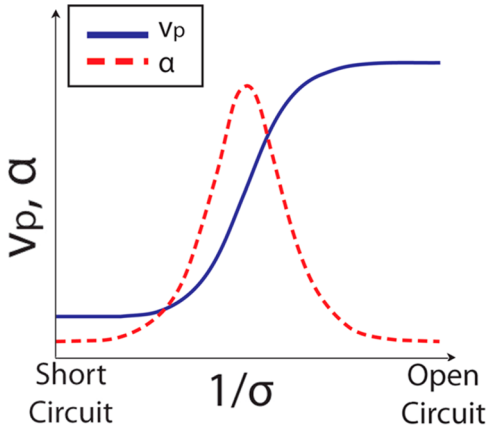

Figure 5. SAW attenuation, α and phase velocity ν_p as a function of thin film resistivity $(1/\sigma)$ for SAW devices .

parameters can be optimized to develop a sensor that operates in the desired nominal film conductivity range, with exposure to increasing vapor concentration either causing the sensor IL to decrease (if sensor operation is on the left, or low resistivity side of the peak) or causing the sensor IL to increase (if sensor operation is on the right, or high resistivity side of the peak) as the film resistivity decreases with increasing vapor concentration. Thus, the double layer Pd nanoparticle coated device was operating on the right side of the attenuation peak (Figure 5). Exposure to 8% H_2 in N_2 caused an increase in conductivity (decrease in resistivity) that caused the sensor operating point to move slightly to the left and up the attenuation curve (Figure 5), increasing device IL with higher concentration. Understanding the interaction of attenuation and film conductivity is essential to properly interpret these device responses.

In order to distinguish between the changes observed due to modifications in conductivity, and due to mass-loading or viscoelastic changes in the sensitive film, devices with metalized delay paths in which conductivity changes would have no effect—called "short-circuit" devices (single and double layer Pd)—were tested before, during, and after exposure to 1600 ppm of H_2 in N_2. It was observed that for the single nanoparticle Pd layer short-circuit SAW device, the reference response did not change upon exposure to hydrogen (Supporting Information,Figure S4 c), and the sensing response (SI Figure S5a) showed a slight decrease in IL (about 0.5 dB) with exposure to hydrogen (roughly as large a change as for the open circuit case, (Figure 4a), and a very slight (0.005 μs) decrease in delay. For the two-layer Pd nanocluster film (SI Figure S5b), the sensor response had a nominal insertion loss that was quite high, at more than 85 dB, and thus any changes caused by exposure to hydrogen or nitrogen purges were somewhat masked by the noise at this low signal level. Changes with exposure to hydrogen were difficult to observe due to the high device IL, although it appears there may have been a decrease in delay and a small increase in IL. It was evident from the behavior of open and short circuit SAW devices that one primary sensing mechanism of the Pd nanoparticle coated SAW devices here was hydrogen induced changes in conductivity of the sensing film. This conclusion was supported by the fact that the two-layer open-circuit devices (Figure 4b) responded to the addition of H_2 with a significant decrease in IL, while the metalized (short-circuit) two-layer device (Figure S5b) did not show a clear IL change in response to hydrogen. A mass or viscoelastic change of the Pd layer would have produced a response on SAWs with both open circuits and short circuits. The decrease in delay in response to hydrogen in the double layer short-circuit Pd nanoparticle film was likely due to a stiffening of the film upon hydrogen exposure, although the changes were somewhat masked by system noise at the high insertion losses seen for the two-layer short-circuit devices. The open-circuit one and two layer Pd film devices produced a reversible increase in reflected peak level of about 1 and 3 dB, respectively. A rather large delay shift of 0.05 μs (50 ns) was observed in the case of the open-circuit two layer film which was not evident for the single layer films (open or short circuit), and was also observed for the short circuit two layer film device.

The most likely explanation for these IL changes is that the conductivity of the two layer Pd nanocluster film was in a range in which the SAW response was sensitive, while single layer films were probably too low in conductivity to produce changes in SAW response with moderate conductivity variations. Delay changes appear to be due to an increase in film stiffness with hydrogen exposure. Additional work would be required to fully characterize the contributions of electrical and mechanical/elastic properties to sensor response. Clearly, the two layer Pd nanoparticle based open circuit SAW devices produced measurable changes when exposed to H_2 and further modification of the film properties could produce optimized sensors with significantly enhanced sensitivity. It should also be

DOI: 10.1021/am507531s
ACS Appl. Mater. Interfaces 2015, 7, 5709−5714

noted that the responses to H_2 exposure and removal were rapid at room temperature.

CONCLUSIONS

Pd nanoparticle based SAW sensors were fabricated that produced measurable changes in response to exposure to hydrogen. Changes in the conductivity of the Pd film upon exposure to hydrogen were found to be a principal mechanism behind the sensing response. Almost complete recovery was obtained once the analyte was removed. The response time of these Pd nanoparticle based SAW sensors was rapid with very little hysteresis. In situ conductivity measurements on similar Pd nanoparticle films confirmed hydrogen induced lattice expansion leading to conductive pathways and changes in conductivity as a primary reason behind the sensitivity to hydrogen. Such a Pd nanoparticle based SAW detection strategy could potentially be extended to other nanomaterials for the purpose of sensing other toxic and explosive analytes.

ASSOCIATED CONTENT

Supporting Information

Materials; preparation of palladium (Pd) nanoparticle solution; characterization of Pd nanoparticles; ultra violet−visible (UV-vis) spectroscopy; transmission electron microscopy; Pd nanoparticle film preparation for conductivity measurements; (Figure S1) characterization of Pd nanoparticles; conductivity measurements; (Figure S2) experimental setup for measuring the conductivity of Pd nanoparticle based films in the presence of hydrogen; fabrication of SAW based H_2 sensors; (Figure S3) design of SAW devices used in this study; measurement of real time response of SAW devices; (Figure S4) measured time domain reference response of SAW sensors before, during and after hydrogen exposure for non metalized open circuit SAW devices; (Figure S5) measured time domain response of SAW sensor with metallized short circuit propagation path coating before, during, and after exposure to hydrogen; and additional references. This material is available free of charge via the Internet at http://pubs.acs.org.

AUTHOR INFORMATION

Corresponding Author

*E-mail: eborguet@temple.edu.

Notes

The authors declare no competing financial interest.

ACKNOWLEDGMENTS

The authors gratefully acknowledge funding provided by NASA (Contract Number NNX11CI26P), NSF instrumentation grant (CHE-0923077) for the JEOL JEM-1400 TEM, and the Army Research Laboratory through contract W911NF-10-2-009.

REFERENCES

(1) Hubert, T.; Boon-Brett, L.; Black, G.; Banach, U. "Hydrogen Sensors" a Review. *Sens. Actuators, B* **2011**, *157*, 329−352.

(2) Grimes, C. A.; Ong, K. G.; Varghese, O. K.; Yang, X.; Mor, G.; Paulose, M.; Dickey, E. C.; Ruan, C.; Pishko, M. V.; Kendig, J. W. A Sentinel Sensor Network for Hydrogen Sensing. *Sensors* **2003**, *3*, 69−82.

(3) Devika, S.; Gilroy, K. D.; Niaux, A.; Boulesbaa, A.; Neretina, S.; Borguet, E. Seeing Is Believing: Hot Electron Based Gold Nanoplasmonic Optical Hydrogen Sensor. *ACS Nano* **2014**, *8*, 7755−7762.

(4) Buvailo, A.; Xing, Y.; Hines, J.; Borguet, E. Thin Polymer Film Based Rapid Surface Acoustic Wave Humidity Sensors. *Sens. Actuators, B* **2011**, *156*, 444−449.

(5) Buvailo, A. I.; Xing, Y.; Hines, J.; Dollahon, N.; Borguet, E. TiO_2/LiCl-Based Nanostructured Thin Film for Humidity Sensor Applications. *ACS Appl. Mater. Interfaces* *3*, 528−533.

(6) Ricco, A. J.; Martin, S. J. Thin Metal Film Characterization and Chemical Sensors: Monitoring Electronic Conductivity, Mass Loading and Mechanical Properties with Surface Acoustic Wave Devices. *Thin Solid Films* **1991**, *206*, 94−101.

(7) Martin, S. J.; Frye, G. C. Surface Acoustic Wave Response to Changes in Viscoelastic Film Properties. *Appl. Phys. Lett.* **1990**, *57*, 1867−1869.

(8) Ricco, A. J.; Martin, S. J.; Zipperian, T. E. Surface Acoustic Wave Gas Sensor Based on Film Conductivity Changes. *Sens. Actuators* **1985**, *8*, 319−333.

(9) Sakintuna, B.; Lamari-Darkrim, F.; Hirscher, M. Metal Hydride Materials for Solid Hydrogen Storage: A Review. *Int. J. Hydrogen Energy* **2007**, *32*, 1121−1140.

(10) Lopez Alonso, N.; Lodziana, Z.; Illas i Riera, F.; Salmeron, M. When Langmuir Is Too Simple: H_2 Dissociation on Pd (111) at High Coverage. *Phys. Rev. Lett.* **2004**, *93*, 146103−1−146103−4.

(11) Pisarev, A. A. Hydrogen Adsorption on the Surface of Metals. In *Gaseous Hydrogen Embrittlement of Materials in Energy Technologies: Mechanisms, Modelling and Future Developments, illustrated ed.*; Elsevier: New York, 2012; Vol. 2, pp 3−26.

(12) Khanuja, M.; Mehta, B.; Agar, P.; Kulriya, P.; Avasthi, D. Hydrogen Induced Lattice Expansion and Crystallinity Degradation in Palladium Nanoparticles: Effect of Hydrogen Concentration, Pressure, and Temperature. *J. Appl. Phys.* **2009**, *106*, 093515.

(13) Lewis, F. A. The Palladium-Hydrogen System. *Annu. Rev. Mater. Sci.* **1967**, *21*, 269−304.

(14) Baldi, A.; Narayan, T. C.; Koh, A. L.; Dionne, J. A. In Situ Detection of Hydrogen-Induced Phase Transitions in Individual Palladium Nanocrystals. *Nat. Mater.* **2014**, *13*, 1143−1148.

(15) Lynch, J. F.; Flanagan, T. B. Dynamic Equilibrium between Chemisorbed and Absorbed Hydrogen in the Palladium/Hydrogen System. *J. Phys. Chem.* **1973**, *77*, 2628−2634.

(16) Adams, B. D.; Chen, A. The Role of Palladium in a Hydrogen Economy. *Mater. Today* **2011**, *14*, 282−289.

(17) Feenstra, R.; Griessen, R.; Groot, D. G. De. Hydrogen Induced Lattice Expansion and Effective H−H Interaction in Single Phase PdH C. *J. Phys. F: Met. Phys.* **1986**, *16*, 1933−1952.

(18) Ingham, B.; Toney, M. F.; Hendy, S. C.; Cox, T.; Fong, D. D.; Eastman, J. A.; Fuoss, P. H.; Stevens, K. J.; Lassesson, A.; Brown, S. A.; Ryan, M. P. Particle Size Effect of Hydrogen-Induced Lattice Expansion of Palladium Nanoclusters. *Phys. Rev. B* **2008**, *78*, 245408−1- 245408−5.

(19) Walter, E.; Favier, F.; Penner, R. Palladium Mesowire Arrays for Fast Hydrogen Sensors and Hydrogen-Actuated Switches. *Anal. Chem.* **2002**, *74*, 1546−1553.

(20) Walter, E.; Penner, R.; Liu, H.; Ng, K.; Zach, M.; Favier, F. Sensors from Electrodeposited Metal Nanowires. *Surf. Interface Anal.* **2002**, *34*, 409−412.

(21) Frazier, G. A.; Glosser, R. Characterization of Thin Films of the Palladium−Hydrogen System. *J. Alloys Compd.* **1980**, *74*, 89−96.

(22) D'Amico, A.; Palma, A.; Verona, E. Surface Acoustic Wave Hydrogen Sensor. *Sens. Actuators* **1983**, *3*, 31−39.

(23) Yamanaka, K.; Nakaso, N.; Sim, D.; Fukiura, T. Principle and Application of Ball Surface Acoustic Wave (SAW) Sensor. *Acoust Sci. Technol.* **2009**, *30*, 2−6.

(24) Mohamed, M.; Moussa, W. A. A Finite Element Model of a MEMS-Based Surface Acoustic Wave Hydrogen Sensor. *Sensors* **2010**, *10*, 1232−1250.

(25) Jakubik, W. P. Investigations of Thin Film Structures of WO_3 and WO_3 with Pd for Hydrogen Detection in a Surface Acoustic Wave Sensor System. *Thin Solid Films* **2007**, *515*, 8345−8350.

DOI: 10.1021/am507531s
ACS Appl. Mater. Interfaces 2015, 7, 5709−5714

(26) Jakubik, W. P.; Urbanczyk, M. W.; Kochowski, S.; Bodzenta, J. Bilayer Structure for Hydrogen Detection in a Surface Acoustic Wave Sensor System. *Sens. Actuators, B* **2002**, *82*, 265−271.
(27) Noh, J. S.; Lee, J. M.; Lee, W. Low-Dimensional Palladium Nanostructures for Fast and Reliable Hydrogen Gas Detection. *Sensors* **2011**, *11*, 825−851.
(28) Khanuja, M.; Varandani, D.; Mehta, B. R. Pulse Like Hydrogen Sensing Response in Pd Nanoparticle Layers. *Appl. Phys. Lett.* **2007**, *91*, 2531211−253121−3.
(29) Aruna, I.; Mehta, B. R.; Malhotra, L. K. Faster H Recovery in Pd Nanoparticle Layer Based Gd Switchable Mirrors: Size-Induced Geometric and Electronic Effects. *Appl. Phys. Lett.* **2005**, *87*, 103101−1- 103101−3.
(30) Sachs, C.; Pundt, A.; Kirchheim, R.; Winter, M.; Reetz, M. T.; Fritsch, D. Solubility of Hydrogen in Single-Sized Palladium Clusters. *Phys. Rev. B* **2001**, *64*, 075408−1- 075408−10.
(31) Pundt, A.; Suleiman, M.; Bähtz, C.; Reetz, M. T.; Kirchheim, R.; Jisrawi, N. M. Hydrogen and Pd-Clusters. *Mater. Sci. Eng., B* **2004**, *108*, 19−23.
(32) Suleiman, M.; Jisrawi, N. M.; Dankert, O.; Reetz, M. T.; Bähtz, C.; Kirchheim, R.; Pundt, A. Phase Transition and Lattice Expansion During Hydrogen Loading of Nanometer Sized Palladium Clusters. *J. Alloys Compd.* **2003**, *356−357*, 644−648.
(33) Eastman, J. A.; Thompson, L. J.; Kestel, B. J. Narrowing of the Palladium-Hydrogen Miscibility Gap in Nanocrystalline Palladium. *Phys. Rev. B* **1993**, *48*, 84−92.
(34) Wolf, R. J.; Lee, M. W.; Ray, J. R. Pressure-Composition Isotherms for Nanocrystalline Palladium Hydride. *Phys. Rev. Lett.* **1994**, *73*, 557−560.
(35) Fichtner, M. Nanotechnological Aspects in Materials for Hydrogen Storage. *Adv. Eng. Mater.* **2005**, *7*, 443−455.
(36) Bhethanabotla, V. R.; Bhansali, S. Surface Acoustic Wave Hydrogen Sensor. Google Patents: 2006.
(37) Sadek, A. Z.; Wlodarski, W.; Shin, K.; Kaner, R. B.; Kalantar-Zadeh, K. A Polyaniline/WO_3 Nanofiber Composite-Based ZnO/64° YX $LiNBO_3$ SAW Hydrogen Gas Sensor. *Synth. Met.* **2008**, *158*, 29−32.
(38) Ramakrishnan, N.; Nemade, H. B.; Palathinkal, R. P. Finite Element Method Simulation of a Surface Acoustic Wave Hydrogen Sensor with Palladium Nano-Pillars as Sensing Medium. *Sens. Lett.* **2010**, *8*, 824−828.
(39) Huang, F. C.; Chen, Y. Y.; Wu, T. T. A Room Temperature Surface Acoustic Wave Hydrogen Sensor with Pt Coated ZnO Nanorods. *Nanotechnology* **2009**, *20*, 065501−1−065501−6.
(40) Penza, M.; Sadek, A. Z.; Zheng, H. D.; Aversa, P.; McCulloch, D. G.; Kalantar-Zadeh, K.; Wlodarski, W. SAW Gas Sensors with Titania Nanotubes Layers. *Sens. Lett.* **2011**, *9*, 925−928.
(41) Phillips, A. B.; Shivaram, B. S. A Technique to Measure Hydrogen Absorption in Isolated Nanometer Structures. *Rev. Sci. Instrum.* **2008**, *79*, 013907−1−013907−4.
(42) Phillips, A. B.; Shivaram, B. S.; Myneni, G. R. Hydrogen Absorption at Room Temperature in Nanoscale Titanium Benzene Complexes. *Int. J. Hydrogen Energy* **2011**, *37* (2), 1546−1550.
(43) Teranishi, T.; Miyake, M. Size Control of Palladium Nanoparticles and Their Crystal Structures. *Chem. Mater.* **1998**, *10*, 594−600.
(44) Naresh, N.; Wasim, F.; Ladewig, B.; Neergat, M. Removal of Surfactant and Capping Agent from Pd Nanocubes (Pd-NCs) Using *tert*-Butylamine: Its Effect on Electrochemical Characteristics. *J. Mater. Chem. A* **2013**, *1*, 8553−8559.
(45) Crespo-Quesada, M.; Andanson, J.-M.; Yarulin, A.; Lim, B.; Xia, Y.; Kiwi-Minsker, L. UV−Ozone Cleaning of Supported Poly (Vinylpyrrolidone) -Stabilized Palladium Nanocubes: Effect of Stabilizer Removal on Morphology and Catalytic Behavior. *Langmuir* **2011**, *27*, 7909−7916.
(46) Ibañez, F. J.; Zamborini, F. P. Ozone- and Thermally Activated Films of Palladium Monolayer-Protected Clusters for Chemiresistive Hydrogen Sensing. *Langmuir* **2006**, *22*, 9789−9796.

DOI: 10.1021/am507531s
ACS Appl. Mater. Interfaces 2015, 7, 5709−5714